

permits the combined RI library search-AR comparison to be implemented in routine organic analysis for the positive peak identification without resorting to GC-MS.

Acknowledgement. This paper was supported by the Korean Science & Engineering Foundation (1988 project number : 881-0304-005-2).

References

1. W. Jennings and T. Shibamoto, "Qualitative analysis of Flavor and Fragrance Volatiles by Glass Capillary Column Gas Chromatography", Academic Press, New York, 1980.
2. K. Tanaka, D. Hine, A. West-dull, and T. B. Lynn, *Cline. Chem.*, **26**, 1839 (1980).
3. A. J. Macleed and N. G. de Troconis, *J. Agric. Food Chem.*, **30**, 515 (1982).
4. R. R. Freemann, T. A. Rooney, and L. H. Altmayer, Technical Paper No. 83, Hewlett-Packard, Avondale, PA.
5. R. J. Phillips, R. R. Wolstromer, and R. R. Freeman, Application Note An 228-16, Hewlett-Packard, Avondale, PA.
6. B. J. Perrio, H. W. Peel, and D. J. Ballantyne, *J. Chromatogr.*, **341**, 81 (1985).
7. M. Y. Tsai, C. Oliphant, and M. W. Josephson, *J. Chromatogr.*, **341**, 1 (1985).
8. M. F. Lefevere, B. J. Verhaeghe, D. M. Declerck, and A. P. deLeernheer, *Biomed. Environ. Mass Spectrum.*, **15**, 311 (1988).
9. K. R. Kim, M. K. Hahn, J. H. Kim, and H. K. Park, Proceedings of the Third Korea-Japan Joint Symposium on Analytical Chemistry, 19-12 April, 119 (1989).
10. C. Wurth, A. Kumps, and Y. Mardens, *J. Chromatogr.*, **491**, 186 (1989).
11. N. W. Davies, *J. Chromatogr.*, **503**, 1 (1990).
12. M. A. Kaiser and F. J. Debbrecht., "Modern Practice of Gas Chromatography", R. L. Grob, ed., Wiley, New York, 1977.
13. E. Kugler, W. Halang, R. Schlenkermann, H. Webel, and R. Langlais, *Chromatographia*, **10**, 438 (1977).
14. K. R. Kim, J. H. Kim, H. K. Park, and C. H. Oh, *Bull. Korean Chem. Soc.*, **12**(1), 87 (1991).
15. G. Schomburg, H. Behlau, R. Dielmann, F. Weeks, and H. Husmann, *J. Chromatogr.*, **142**, 87 (1977).
16. G. Schomburg, H. Husmann, and R. Rittmann, *J. Chromatogr.*, **204**, 85 (1981).
17. K. Grob, Jr. and R. Mueller, *J. Chromatogr.*, **244**, 185 (1982).

Structural Transition of A-Type Zeolite: Molecular Dynamics Study

Mee Kyung Song* and Hakze Chon†

Division of Chemistry, Korea Institute of Science and Technology, P.O.Box 131, Cheongryang, Seoul 130-650

†Department of Chemistry, Korea Advanced Institute of Science and Technology, Taejon 305-338

Received October 13, 1992

Molecular dynamics (MD) calculations were carried out in order to investigate the effect of MD cell size to predict the melting phenomena of A-type zeolite. We studied two model systems: a pseudocell of $(T_2O_4Na)_n$ ($L=12.264$ Å, $N=84$) and a true-cell of $(SiAlO_4Na)_n$ ($L=24.528$ Å, $N=672$), where T is Si or Al. The radial and bond angle distribution functions of T(Si, Al)-O-T(Si, Al) and diffusion coefficients of T and O were reported at various temperatures. For the true-cell model, the melting temperature is below 1500 K and probably around 1000 K, which is about 600-700 K lower than the pseudocell model. Although it took more time (about 30 times longer) to obtain the molecular trajectories of the true-cell model than those of the pseudocell model, the true-cell model gave more realistic structural transition for the A-type zeolite, which agrees with experiment.

Introduction

In molecular dynamics (MD) simulations, the Newtonian equations of motion are solved numerically for a set of N particles in volume V .¹ Usually, as in Monte Carlo simulations,^{2,3} periodic boundary conditions are used to approximate an infinite system. The advantage of the MD approach is that one can study time depended single particle properties such as self-diffusion coefficients and the correlation functions. Recently, the extension of MD methods to treat ensembles other than the traditional microcanonical ensemble has attracted considerable attention.⁴⁻⁶ And the use of La-

grangian which allows the variation of the MD cell shape has demonstrated its usefulness in applications to structural changes in solid state.⁷⁻⁹

The melting phenomena of A-type zeolite with temperature changes were studied.^{10,11} But the temperature of the structural transition (2100 K) was higher than the experimental result (1100 K). In this study, the effect of the MD cell size on the prediction of the melting phenomena of A-type zeolite is investigated. Using the (N, V, E) ensemble the radial distribution functions and the related properties were calculated for a true-cell model of $(SiAlO_4Na)_n$ ($L=24.528$ Å, $N=672$) at 298, 900, 1500 and 2100 K. And a comparative discussion

is made for the results of the model calculations of the true-cell and pseudocell.

Method of Calculations

Model Compounds and Computational Details. To investigate the effect of MD cell size on the prediction of the melting phenomena of A-type zeolite, the true-cell model (SiAlO_4Na)_n, which has the cell length of $L=24.528$ Å with the number of particles of $N=672$ has been studied. MD calculations of the pseudocell model ($\text{T}_2\text{O}_4\text{Na}$)_n, which has $L=12.264$ Å and $N=84$, were previously studied.^{10,11} The numbers of atoms of T, O, and Na are 24, 48, and 12 for the pseudocell model and are 192, 384, and 94 for the true-cell model respectively. The charge of each atom was described previously.¹² At the beginning of each simulation, used X-ray positions¹³ for the coordinates of the framework we atoms (T, O) and Na ions and let the velocities of the atoms have Boltzmann distributions at the simulation temperatures of 298, 900, 1500, and 2100 K. We used the effective pairwise interatomic potentials and the periodic boundary conditions. The classical equations of motions were integrated with Verlet's finite difference algorithm.¹⁴ A very short time step ($\Delta t=1.0\times 10^{-15}$) was used in order to effectively integrate the equations of motion. About 2000 time steps were used to equilibrate the systems. Further, another 500 time step trajectory was discarded in the averaging procedure. Approximately 3s CPU time was required for one step run of the true-cell model ($N=672$) on a CRAY-2S supercomputer, which took about thirty times longer than the for the pseudocell model ($N=84$). During the constant energy runs (for 10000 time steps, namely, 10 ps), the temperature of the atoms fluctuated around each simulation temperature, and their fluctuations increased as the temperature increased.

In experiment, all types of zeolites decompose when they stay a long time in air. To test that property, 50000 time step (50 ps) of MD calculations were performed at 900 and 1500 K. but there was no difference in rdf shape and peak height for 10000 and 50000 time step calculations. Therefore, we think the Brownian dynamics^{15,16} is useful to study that phenomena. This will be our future study.

Interatomic Potential Functions. The pairwise effective interatomic potentials used here are the same with those in the previous calculation.¹⁰ The potentials include the electrostatic, polarization, dispersion, repulsion, and Morse potentials.

$$V = V_{el} + V_{pol} + V_{d-r} + V_{T-O} \quad (1)$$

Details of the potential functions were described in reference 10.

Results and Discussion

Structural transition with temperature change may be predicted from the calculations of the structural factors such as radial distribution function (rdf) and T-O-T bond angle distribution functions.

Figure 1 shows the calculated rdf of T-O, T-T, O-O, Na-O, and Na-T pairs for the true-cell model at four different temperatures. The peak height becomes lower as the tem-

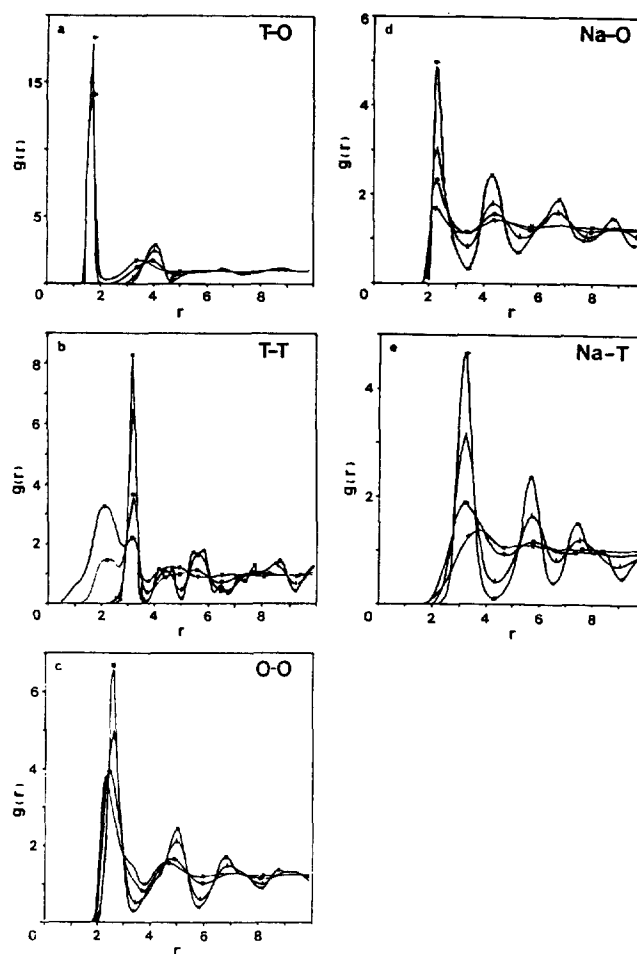


Figure 1. Radial distribution functions of (a) T-O, (b) T-T, (c) O-O, (d) Na-O, and (e) Na-T pairs in A-type zeolite (for true-cell model; $L=24.528$ Å, $N=672$) with temperatures of 298 (■), 900 (▲), 1500 (●), and 2100 (☆) K, r is in Å.

perature increases, and finally the shift of the peak positions are observed at 1500 K. With increasing temperature, the decrease in the height of the peak maxima and width of the rdf indicates the disorder of the structure due to increased thermal motions. For T-O pair, the second-nearest-neighbor distance diminished, while for T-T and O-O pairs the first-nearest-neighbor distance decreased. This indicates a large distortion of the tetrahedron structure along with the change of the symmetry of A-type zeolite. The rdf changes are prominent at 2100 K. Namely, as the temperature increases, the zeolite structure becomes unstable, then the structural transition occurs. For Na-O pair, the nearest-neighbor distance changed little, but the first Na-T peak becomes large at 2100 K due to van der Waals repulsion.

Figure 2 shows the calculated T-O-T bond angle distribution functions for the true-cell model with respect to temperature. As the temperature increases, the peaks are broadened, reducing the probability of finding the bond angles. Broad distribution of bond angles appeared around 150° . At 1500 K the peak around 150° becomes much lowered, and a new peak around 75° appears with the same probability of finding the bond angles. This new peak around 75° is found with higher probability at 2100 K than at 1500 K.

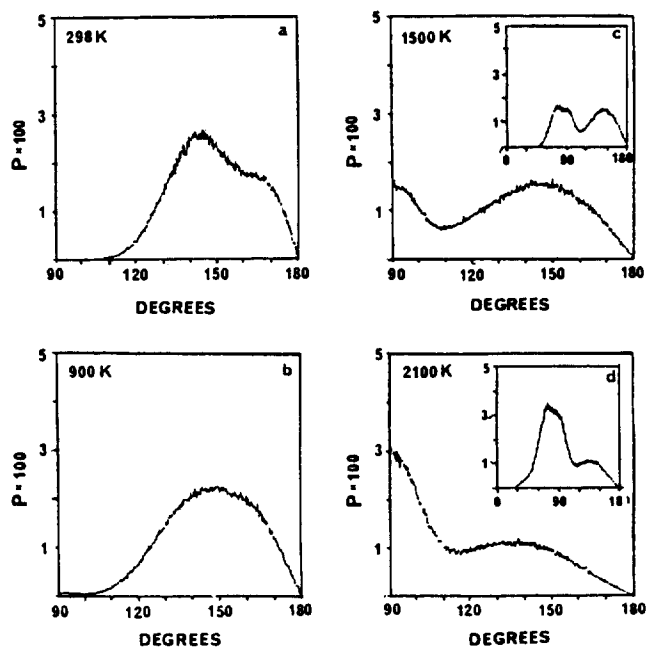


Figure 2. Distributions of (Si, Al)T-O-T(Si, Al) bond angles for A-type zeolite at (a) 298 (b) 900 (c) 1500 and (d) 2100 K. The y-axis gives the probability per degree of finding the indicated bond angles. The inset provides the same feature except the range of the x-axis, namely, from 0 to 180°.

It means that the original geometry of A-type zeolite disappeared and many portions of zeolite framework are destroyed. From the MD results of rdf and bond angle distribution functions of the true-cell model we identify that the transition temperature is around 900-1500 K region. It was 1500-2100 K region when the pseudocell model^{10,11} was used. Experimentally, the structural transition of A-type zeolite into a cristobalite-type structure occurs at 1073 K. This agrees well with the true-cell model, *i.e.*, when $L=24.528 \text{ \AA}$ and $N=672$. Using the true-cell model, the structural transition of A-type zeolite is in reasonable agreement with the experimental result.

The diffusion coefficient of the framework atoms and Na ions at each temperature was determined from the plot of a mean-square displacement versus time using Einstein relation ($D=1/6 \delta \langle |r(t) - r(0)|^2 \rangle / \delta t$). In order to obtain the more reproducible figures during each run, the positions and velocities of all atoms were written every eight time step on a disk file and averaged over all possible starting configurations. Figure 3 is another representation of phase transition of A-type zeolite. It is the plot of $\log D$ versus $1/T(K)$. The phase transition occurs when the slope change exists. There are slope differences in this figure at around 1.0 $1/T(K)$ for the true-cell and 0.6 $1/T(K)$ for the pseudocell model for the framework T and O atoms. The temperatures are 1000 K and 1700 K, respectively. They are the framework T and O atoms which constitute the zeolite structure. As the Na ions only occupy the interstitial sites of zeolite, it may be ruled out in determining the phase transition of zeolite using the plot of $\log D$ versus $1/T(K)$. Now, this can be a clear evidence of phase transition of zeolite A. Namely, the phase transition occurs at around 1000 K and 1700 K

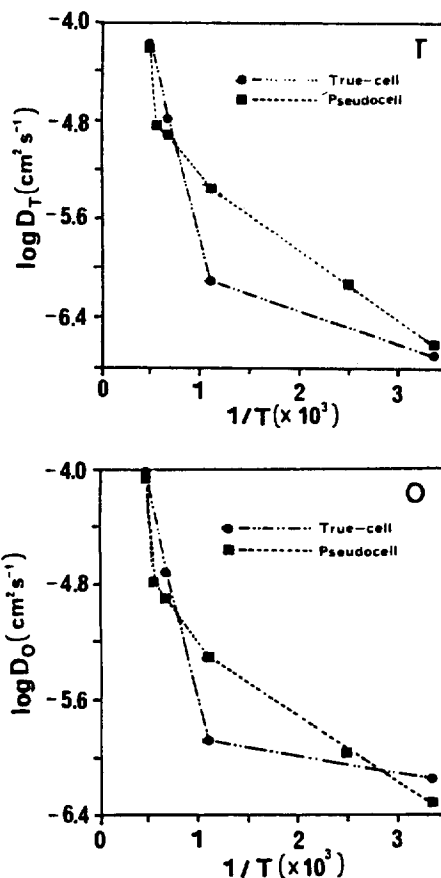


Figure 3. Diffusion coefficients of framework T and O atoms for true-cell (—•—) and pseudocell (---■---) models at each temperature. The plot is $\log D$ versus $1/T(K)$.

for true-cell and pseudocell model, respectively.

In conclusion, the structural transition of A-type zeolite based on the true-cell model shows more realistic result. Though the calculations for the true-cell model require more time in obtaining the molecular trajectories, the predicted structural transition of A-type zeolite is in reasonable agreement with the experiment.

References

1. B. J. Alder and T. W. Wainright, *J. Chem. Phys.*, **27**, 1208 (1957).
2. N. Metropolis, A. W. Rosenbluth, M. N. Rosenbluth, and A. H. Teller, *J. Chem. Chem.*, **21**, 1087 (1953).
3. A. J. Barker and R. O. Watts, *Phys. Lett.*, **3**, 144 (1969).
4. H. C. Andersen, *J. Chem. Phys.*, **72**, 2384 (1980).
5. M. Parrinello and A. Rahman, *Phys. Rev. Lett.*, **45**, 1196 (1980).
6. M. Parrinello and A. Rahman, *J. Appl. Phys.*, **52**, 7182 (1981).
7. S. Nose and M. L. Klein, *J. Chem. Phys.*, **78**, 6928 (1983).
8. R. G. Munro and R. D. Mountain, *Phys. Rev. B* **28**, 2261 (1983).
9. J. S. Lee, M. K. Song, H. Chon, and M. S. Jhon, *Bull. Korean Chem. Soc.*, **12**, 490 (1991).
10. M. K. Song, J. M. Shin, H. Chon, and M. S. Jhon, *J.*

- Phys. Chem.*, **93**, 6463 (1989).
11. M. K. Song, H. Chon, and M. S. Jhon, *J. Phys. Chem.*, **94**, 7671 (1990).
 12. M. K. Song, K. T. No, H. Chon, and M. S. Jhon, *J. Mol. Catal.*, **47**, 73 (1988).
 13. R. L. Yanagida, A. A. Amaro, and K. Seff, *J. Phys. Chem.*, **77**, 805 (1973).
 14. L. Verlet, *Phys. Rev.*, **159**, 98 (1968).
 15. D. L. Ermak and J. A. McCammon, *J. Chem. Phys.*, **69**, 1352 (1978).
 16. E. Dickinson, S. A. Allison, and J. A. McCammon, *J. Chem. Soc. Faraday Trans. 2*, **81**, 591 (1985).

Two Crystal Structures of Dehydrated Fully Ca²⁺-Exchanged Zeolite A Reacting with Rubidium Vapor

Seong Hwan Song and Yang Kim*

Department of Chemical Engineering, Dongseo University, Pusan 616-012

**Department of Chemistry, Pusan National University, Pusan 609-735*

Received October 20, 1992

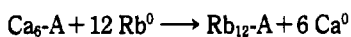
Two single crystals of fully dehydrated Rb⁺-exchanged zeolite A have been prepared by the reduction of all Ca²⁺ ions in dehydrated Ca₆-A by rubidium vapor. Their structures were determined by single crystal X-ray diffraction methods in the cubic space group *Pm3m* ($a=12.160(2)$ Å and $12.166(2)$ Å) at 22(1)°C. In these structures, 12.4(2) to 13.3(2) Rb species are found per unit cell, more than 12 Rb⁺ ions needed to balance the anionic charge of the zeolite framework, indicating that the sorption Rb⁰ has occurred. In each structure, three Rb⁺ ions per unit cell are located at the centers of the 8-rings. Six to eight Rb⁺ ions are found opposite the 6-rings on threefold axes, and three Rb⁺ ions are found in a sodalite unit. About 0.5 Rb⁺ ion lies opposite a 4-ring. The structural analysis indicates the presence of a triangular rubidium cluster in the sodalite cavities. The triangular rubidium clusters may be stabilized by the coordination to two and/or three rubidium ions in the large cavity. Therefore, this cluster may be viewed as (Rb₃)⁴⁺ and/or (Rb₆)⁴⁺.

Introduction

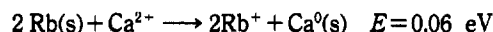
During the past decade, a series of attempts had failed to achieve the fully Rb⁺-exchanged zeolite A.^{1,2} Seff *et al.* reported that large monovalent Rb⁺ ions exchanged incompletely into zeolite A by flow methods.^{1,2} In dehydrated eleven-twelfths Rb⁺-exchanged zeolite A, three equivalent Rb⁺ ions lie at the center of the oxygen 8-rings, and five equivalent Rb⁺ ions lie on threefold axes opposite the 6-rings in the large cavity. The remaining three Rb⁺ ions are non-equivalent and lie on each different threefold axis of unit cell. One Na⁺ ion lies almost at the center of a 6-ring.¹

Recently, fully Cs⁺-exchanged zeolite A has been synthesized by the reduction of all of the Na⁺ ions in Na₁₂-A by cesium vapor.^{3,4} The redox reaction goes to completion at 250°C with 0.1 torr of Cs⁰ to give Cs₁₂-A·1/2Cs. In this structure, each extra Cs atom associates with two or three Cs⁺ ions to form linear (Cs₃)²⁺ or (Cs₄)³⁺ clusters. These clusters lie on threefold axes and extend through the centers of sodalite units.

This work was initiated with the hope that the intrazeolitic redox potential for the reaction



would be positive at the conditions employed to result in complete exchange. The *E* values, not involving the zeolite, are easily calculated.⁵



The resulting material may be of interest because the volume of the exchangeable cations would be large and some extra Rb⁰ atoms may be present, forming Rb clusters as were Cs⁰ atoms in the structure of the dehydrated Na₁₂-A reacted with cesium. These extra Rb atoms are likely to complex to Rb⁺ cations to form rubidium clusters.

Experimental

Single crystals of zeolite 4A were prepared by Charnell's methods⁶ using seed crystals from a previous synthesis. A single crystal about 0.085 mm on an edge was lodged in a fine glass capillary. To prepare Ca₆-A, an exchange solution of 0.04325 M Ca(NO₃)₂ (Aldrich, 99.997%) and 0.00675 M CaO (Aldrich, 99.995%) with a total concentration of 0.05 M was allowed to flow past each crystal at a velocity of approximately 1.0 cm/sec for 3 days at 21(1)°C. The crystals remained colorless.

The hydrated fully Ca²⁺-exchanged zeolite A was dehydrated at 360°C and 2×10⁻⁶ Torr for 2 days. Rubidium vapor was introduced by distillation from a side-arm break-seal ampoule to the glass-tube extension of the crystal-containing capillary. This glass reaction vessel was then sealed off under vacuum placed within a pair of cylindrical horizontal oven, axis colinear, attached. The oven about crystal was